ELSEVIER

Journal of Photochemistry and Photobiology A: Chemistry 145 (2001) 23–34

Journal of Photochemistry and Photobiology A:Chemistry

www.elsevier.com/locate/jphotochem

# Origin of the stabilization energy of perylene excimer as studied by fluorescence and near-IR transient absorption spectroscopy

Ryuzi Katoh [a,*], Subrata Sinha [a], Shigeo Murata [a], M. Tachiya [b]

[a] *Photoreaction Control Research Center, National Institute of Advanced Industrial Science and Technology (AIST), 1-1-1 Higashi, Tsukuba, Ibaraki 305-8565, Japan*

[b] *National Institute of Advanced Industrial Science and Technology (AIST), 1-1-1 Higashi, Tsukuba, Ibaraki 305-8565, Japan*

Received 10 April 2001; received in revised form 21 May 2001; accepted 14 June 2001

**Abstract**

The origin of the stabilization energy of perylene excimer in toluene has been studied. In order to measure the fluorescence spectra and its decay profiles under the condition free from the reabsorption effect, we designed a thin optical cell with a path length of about 10 μm. From the results, the photophysical parameters of perylene excimer such as the formation rate constant, the peak position and the lifetime and the quantum yield of fluorescence can be obtained. Using these values, the binding energy of perylene excimer can be evaluated as 0.44 eV from the temperature dependence of the transient absorption. By analyzing the band shape of the charge transfer absorption in near-IR wavelength range, the transfer integral $V$ between a neutral excited state and an ion-pair state can be estimated as 0.37 eV. From these results, we conclude that the stabilization energy of perylene excimer consists of two components: exciton interaction (70%) and charge transfer interaction (30%). We also discuss the origin of the stabilization energy of other aromatic excimers on the basis of the results on perylene excimer. 

*Keywords:* Perylene; Excimer; Excimer fluorescence; Transfer integral; Near-IR transient absorption

## 1. Introduction

Excimer is a complex formed between excited and ground state molecules. It has been studied for many aromatics [1,2]. The formation and decay processes of excimers can be studied by observing the characteristic excimer fluorescence, which is red-shifted as compared to the monomer fluorescence and is broad and structureless. Excimer seems to be a good example for studying the intermolecular interaction in the excited states.

Fig. 1 shows the schematic diagram of the energy levels of excimer on the basis of theoretical considerations [3–5]. The $(M + M^*)$ state is destabilized at short distances by the repulsion energy $E_R$. At the same time, at short distances, the excited state is delocalized among two molecules and the energy level splits into two exciton states by the exciton interaction, i.e., resonance interaction between two electronic configurations, $M^*M$ and $MM^*$. The energy separation between two exciton states is twice that of exciton interaction energy $E_S^{exc}$. In addition to the exciton interaction, the charge transfer interaction between the exciton state and an ion-pair state is also important. The stabilization energy $E_S^{CT}$ by the charge transfer interaction becomes pronounced, when the energy difference $E_0$ between the exciton state and the ion-pair state is small. If the sum of the stabilization energies $(E_S^{exc} + E_S^{CT})$ exceeds the repulsion energy $E_R$, excimer can be formed. The binding energy $E_B$ can be defined as

$$E_B = E_S^{exc} + E_S^{CT} - E_R \quad (1)$$

The lowest energy state of the excimer emits characteristic fluorescence. On the contrary, the higher excited state of the excimer can be studied by observing the absorption from the fluorescent state. Accordingly, combination of fluorescence and transient absorption spectroscopy are important to study the origin of the stabilization energy of excimers. Few attempts have been carried out experimentally to understand the origin of the stabilization energy of excimers [1,5].

Here, we study perylene excimer in toluene. Perylene molecule has a considerably low ionization potential (7.0 eV [6]) and a high electron affinity (1.1 eV [6]). Therefore, a large contribution of the charge transfer interaction to the stabilization energy of its excimer can be expected. Another interesting feature of perylene is opto-electronic functions. Some derivatives of perlyene have been applied for the photocarrier generating pigments [7] and dye-sensitized solar

* Corresponding author. Tel.: +81-298-61-4517; fax: +81-298-61-4840.
*E-mail address:* r-katoh@aist.go.jp (R. Katoh).

1010-6030/01/$ – see front matter 
PII: S1010-6030(01)00562-7

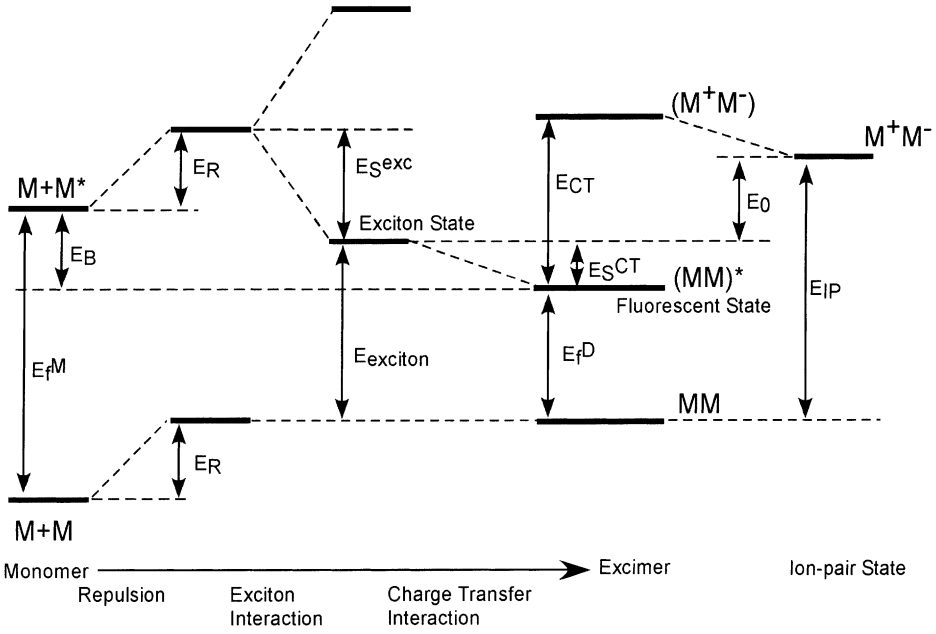


Fig. 1. Energy level diagram for interaction of excimer.

cells [8]. These remarkable functions are ascribed to the charge transfer character of the lowest excited state [9,10]. Thus, we consider that the study of the electronic structure, especially the charge transfer character, of perylene excimer is important to understand these functions in detail.

The formation and decay processes of excimers have been studied mainly by observing the characteristic excimer fluorescence spectra [1]. For perylene in fluid solution, it is difficult to study photophysical processes by fluorescence spectroscopy. Excimer fluorescence of perylene in fluid solution is known to be very weak [11], whereas it can be detected in crystals [12], rigid matrices [13] and LB-films [14]. Although almost no excimer fluorescence of perylene is observed in fluid solution, the presence of the excimer in fluid solution has been confirmed through the measurement of transient absorption [15,16]. This implies that perylene excimer has a low quantum yield of fluorescence. The low solubility of perylene is also a problem for observing the fluorescence of perylene excimer. For pyrene solution, which is the most popular system for observing excimer fluorescence, the excimer fluorescence becomes dominant in solutions at concentrations above $10^{-2}$ M [1], whereas the solubility of perylene in toluene is approximately $5 \times 10^{-3}$ M.

In order to study photophysical processes of excimer, concentrated solutions have to be used. In the case of concentrated solutions (>$10^{-4}$ M), the reabsorption effect affects the fluorescence measurements resulting in the reduction of the intensity in the short wavelength range of the spectrum. Also, the lifetime in the longer wavelength range is seemingly longer than that in the shorter wavelength range. This is because the primary photons emitted from excited molecules are absorbed by other solute molecules and, subsequently, these molecules emit fluorescence again. Many methods have been used to eliminate the reabsorption effect, i.e., the front surface excitation and observation [1,17], the correction using a theoretical model [18]. However, these methods are not sufficient to eliminate the reabsorption effect. In our opinion, the measurement using a thin cell is the best option to eliminate the reabsorption effect and has yielded good results for the measurement of fluorescence lifetime and spectrum [19,20]. In practice, however, it is difficult to design a thin cell for precise measurements. In particular, it is difficult to degas the sample solution in the thin cell. Degassing the sample solution is important to minimize the quenching by oxygen. In order to study the photophysical processes of perylene excimer, the precise fluorescence measurement techniques need to be developed.

Transient absorption spectroscopy is one of the powerful tools for probing excited states. The absorption spectrum of perylene excimer in solution was measured through transient absorption spectroscopy and was reported in the visible wavelength range [15] and in the near-IR range [16]. In the visible range, the spectrum is similar to that of monomer excited state. Therefore, this band can be assigned to the transition from the fluorescent state to the locally excited state of perylene. On the contrary, in the near-IR range the characteristic absorption band of excimer can be observed. This band was assigned to the charge transfer transition from the fluorescent state to the ion-pair state [16]. This charge transfer absorption band reflects the electronic coupling between these states directly. Hence, the electronic structure of excimer can be studied by observing the near-IR absorption band.

In this paper, we study the origin of the stabilization energy of perylene excimer in toluene through fluorescence and transient absorption spectroscopy. In order to measure

the fluorescence spectra and its decay profiles under the condition free from the reabsorption effect, we designed a thin optical cell with a path length of about 10 μm. From these results, we obtained several photophysical parameters; the excimer formation rate constant, the peak position, the quantum yield and the lifetime of the excimer fluorescence. We found that the formation of perylene excimer is almost diffusion-controlled. From the measurements of transient absorption spectra at various temperatures, the binding energy of perylene excimer can be estimated as $E_B = 0.44$ eV. In the near-IR wavelength range, the charge transfer absorption band of excimer can be observed. By analyzing the band shape, the transfer integral $V$ between a neutral exciton state and an ion-pair state can be estimated as $V = 0.37$ eV. From these results, we conclude that the stabilization energy of perylene excimer consists of two components: exciton interaction (70%) and charge transfer interaction (30%). We also discuss the origin of the stabilization energy of other aromatic excimers on the basis of the results on perylene excimer.

## 2. Experimental

Perylene (Wako, GR-grade) was purified by recrystallization. Toluene (Wako, GR-grade) was used as solvent without further purification. Steady-state absorption and emission measurements were carried out with absorption (Shimadzu, UV–Vis 2200) and fluorescence (Hitachi, 850) spectrophotometers, respectively. The spectral response of the fluorescence spectrophotometer was corrected with a standard lamp (Ushio, JPD 100V500WCS). Fluorescence decay curves were obtained by time-correlated single photon counting. The apparatus already described elsewhere [21] was used. The FWHM of the response function of the apparatus was about 60 ps. All the fluorescence measurements were made at 293 K. To eliminate the reabsorption effect, the fluorescence measurements were carried out using a thin optical cell. Fig. 2 shows the thin cell we have constructed. Exciting light irradiates the sample solution placed between the two quartz windows and fluorescence emitted from the thin solution layer is detected. One of the quartz windows (40 mm in diameter) is attached to the front flange by an epoxy resin and the other is attached to one end of the stainless steel flexible tube. The thickness of the cell can be varied by changing the spacer (stainless steel foil) and the minimum thickness attainable is about 10 μm. The other end of the flexible tube is fixed to the back flange. Thus, the absorption spectrum of the thin layer can also be measured using this cell. Teflon coated o-rings were used as gaskets to make the whole cell vacuum-tight. To prepare a sample solution in the cell, the cell is first evacuated with a vacuum pump and then the solution already degassed is introduced from a container connected to the cell. In this way, the thin space between the windows can be filled with the sample solution. The thickness of the sample solution can be determined precisely by measuring the absorption spectrum. In fact, the thickness of the sample solutions was determined to be 50 and 12 μm, respectively, when 50 and 10 μm thick spacers were used.

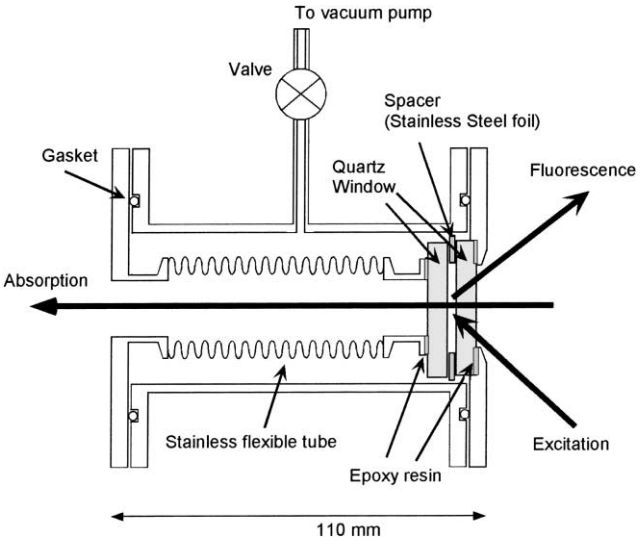


Fig. 2. Thin optical cell for eliminating the reabsorption effect.

For the transient absorption measurements, the 3rd harmonic pulse (355 nm) from a $Nd^{3+}$:YAG laser (Continuum, Surelite II) was used as the pumping light. The pulse duration of the laser was 8 ns. A Xe flash lamp (Hamamatsu, L4642, 2 μs pulse duration) was used as the probe light source. In the visible range, the spectrum of the probe light transmitted through the sample was recorded simultaneously with a gated CCD camera (Roper Scientific, ICCD-MAX) after being dispersed with a monochromator (Roper Scientific, SP-308) controlled with a computer. In the near-IR range (800–2400 nm), the probe light was detected with a photodiode after passing through a monochromator (JASCO, CT-10 for shorter wavelength range (600–1000 nm) and Ritsu, MC-10N for longer wavelength range (900–2400 nm)). A Si-photodiode (Hamamatsu, S-1722) was used for detection in the range 550–950 nm, an InGaAs-photodiode (Hamamatsu, G3476-05) for 900–1600 nm range and an MCT-photodetector (Dorotek, PDI-2TE-4) for 1200–2400 nm range. Signals were processed with a digital oscilloscope (Tektronix, TDS680C) and analyzed with a computer. The temperature of the sample solution in a cell was controlled by circulation of water in a sample holder maintained in a thermostat (Advantec, LCH-4V).

## 3. Results and discussion

### 3.1. Elimination of the reabsorption effect

Fig. 3 shows the steady-state absorption and fluorescence spectra of perylene in toluene under various conditions. In this wavelength range, only the monomer fluorescence can

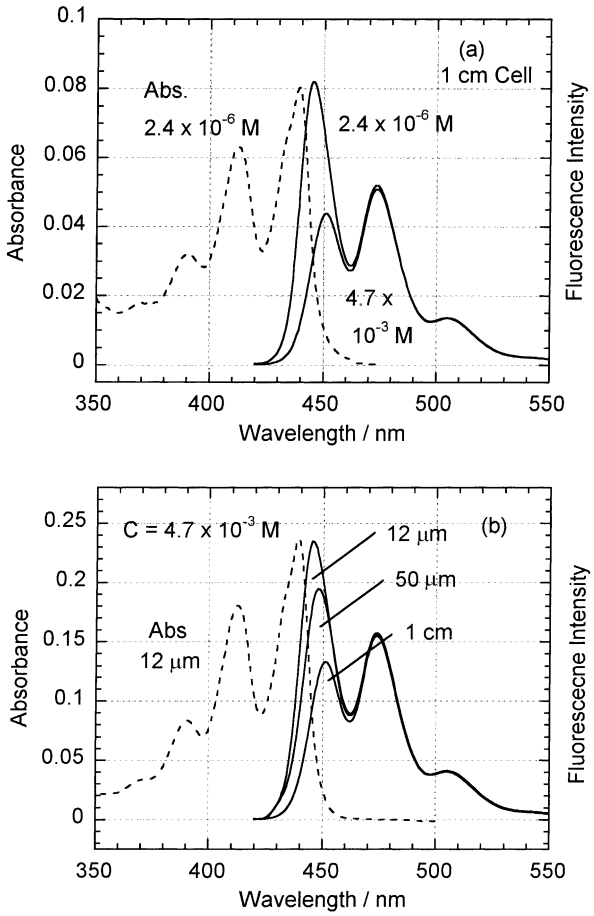


Fig. 3. Absorption and fluorescence spectra of perylene in toluene: (a) absorption and fluorescence spectra in a 1 cm cell of a dilute ($2.4\times10^{-6}$ M) and a concentrated ($4.7\times10^{-3}$ M) solutions; (b) fluorescence spectra of a concentrated ($4.7\times10^{-3}$ M) solution in thin cells with thicknesses of 50 and 12 μm. The absorption spectrum is recorded with the 12 μm cell.

be expected as will be shown in Section 3.3. The spectra using a conventional 1 cm optical cell are shown in Fig. 3(a). Excitation and detection were made at the front surface of the cell. Since the fluorescence spectrum is overlapped significantly with the absorption spectrum around 440 nm, the reabsorption effect is expected in this range. A dilute ($2.4\times10^{-6}$ M) solution seems to be free from the reabsorption effect. In a concentrated solution ($4.7\times10^{-3}$ M) the relative intensity of the short wavelength part of the fluorescence spectrum is reduced. It should be noted that the reabsorption effect is significant even when excitation and detection are made at the front surface of the cell. Fig. 3(b) represents the spectra of concentrated solutions ($4.7\times10^{-3}$ M) recorded using the thin cell with 50 and 12 μm thicknesses. The fluorescence spectrum using the 1 cm cell is also shown for comparison. When the 12 μm cell is used, the absorbance around 440 nm is low and the reabsorption effect is considered to be unimportant. In fact, the spectrum of the 12 μm cell is identical to that of the dilute solution ($2.4\times10^{-6}$ M). This clearly shows that the reabsorption effect is effectively eliminated using the thin cell.

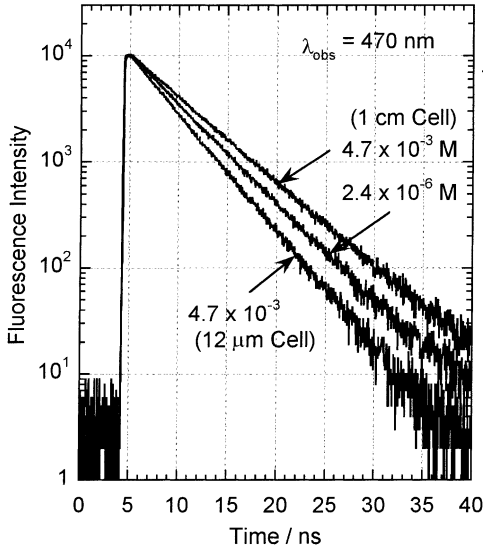


Fig. 4. Fluorescence decay profiles of a dilute solution ($2.4\times10^{-6}$ M) and a concentrated solution ($4.7\times10^{-3}$ M) of perylene in toluene observed at 470 nm in the 1 cm cell and the 12 μm cell.

### 3.2. Rate constant of excimer formation

In many aromatic molecules, the monomer fluorescence lifetime decreases with increasing concentration of solution, which is due to the de-excitation of excited molecules by ground state molecules (self-quenching). Fig. 4 shows the decay profile observed at 470 nm of a dilute solution ($2.4\times10^{-6}$ M) and a concentrated solution ($4.7\times10^{-3}$ M) obtained with the 1 cm cell and the 12 μm cell at 293 K. The lifetime of the concentrated solution in the 12 μm cell is shorter than that of the dilute solution. This clearly shows that the self-quenching occurs in the concentrated solution. Actually, the lifetime of the concentrated solution depends on the cell thickness. In fact, the lifetime of the concentrated solution in 1 cm cell is longer than that of the dilute solution. This clearly shows that the decay kinetics of fluorescence is affected by the reabsorption effect.

There are three main possible mechanisms for the self-quenching of monomer fluorescence, i.e., photochemical reaction, electron transfer, and excimer formation. In the case of anthracene, self-quenching occurs but almost no excimer fluorescence has been observed in concentrated solutions [1]. This is due to the photodimerization between the excited and the ground state molecules. In the present study, however, perylene is stable during the measurements and, therefore, self-quenching by photochemical reaction can be ruled out. Contribution of the electron transfer reaction to the self-quenching can be checked by considering the free energy change $\Delta G$ before and after electron transfer. According to the study by Rehm and Weller [22], fluorescence quenching does not occur efficiently in the case of positive $\Delta G$. As we will discuss in Section 3.6, an ion-pair state (charge separated state) is located above the fluorescent state of excimer. This indicates that the free energy change

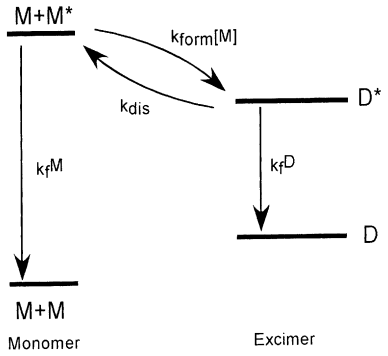


Fig. 5. Rate processes of the monomer excited state and the excimer of perylene.

for the electron transfer reaction is positive. Accordingly, the self-quenching by electron transfer is not efficient. Thus, excimer formation is most likely as the mechanism of self-quenching of perylene monomer fluorescence.

Fig. 5 shows the formation and the dissociation of the excimer $D^*$ by the reaction of the excited molecule $M^*$ with the ground state molecule M. In Fig. 5, $k_{form}$ and $k_{dis}$ represent the rate constants of formation and thermal dissociation of excimer, respectively, and $k_f^M$ and $k_f^D$ are the rate constants of fluorescence decay (inverse of the lifetime) of monomer and excimer, respectively. As shown in Fig. 4, the fluorescence decay recorded at 293 K can be fitted by single exponential function so that the dissociation of $D^*$ into $M^*$ can be neglected at this temperature. Therefore, using the Stern–Volmer relation, the rate constant of fluorescence decay $k_f^M$ (inverse of the fluorescence lifetime $\tau_f^M$) including excimer formation can be expressed as

$$k_f^M = k_f^{M_0} + k_{form}[M] \quad (2)$$

where $k_f^{M_0}$ is the rate constant of fluorescence decay (inverse of the fluorescence lifetime $\tau_f^{M_0}$) in the absence of excimer formation and [M] the concentration of the solution. Accordingly, $k_{form}$ can be obtained from the measurement of $\tau_f^M$ at several concentrations.

We measured the fluorescence lifetimes of perylene solutions at various concentrations and at three different wavelengths (445, 470 and 500 nm) using the 1 cm and the 12 μm cells. The results are listed in Table 1. For a dilute solution ($2.4 \times 10^{-6}$ M) in the 1 cm cell, the fluorescence lifetimes

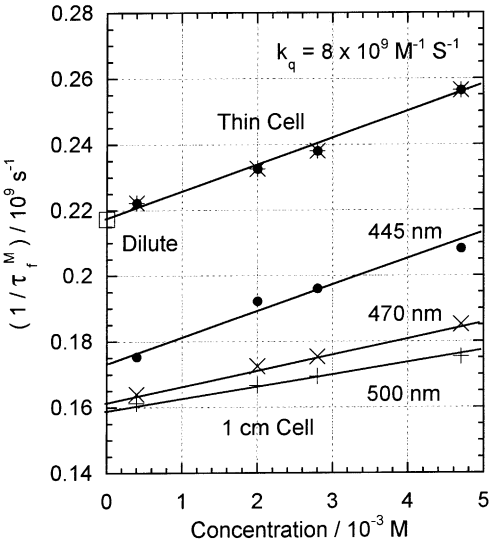


Fig. 6. The Stern–Volmer plot of fluorescence decay rate constants in a 1 cm cell and a 12 μm cell.

are the same (4.6 ns) at the three different wavelengths. This is consistent with the fact that the reabsorption effect is not detected in the fluorescence spectrum at this concentration. Accordingly, we can take the fluorescence lifetime of the dilute solution as the lifetime $\tau_f^{M_0}$ in the absence of excimer formation (see Eq. (2)).

For concentrated solutions ($0.4–4.7 \times 10^{-3}$ M) in the 1 cm cell, the lifetimes are longer than that in the most dilute solution and increase with increasing observation wavelength. Within the concentrated solutions, the lifetime decreases with increasing concentration. This clearly shows that excimer formation occurs. Fig. 6 represents the Stern–Volmer relation at different observation wavelengths in the 1 cm cell. As seen from Fig. 6, the slope changes with the observation wavelength for the 1 cm cell and the lifetimes obtained by extrapolating the plots to the zero concentration do not coincide with the value of the dilute solution. Thus, it is impossible to obtain $k_{form}$ by measuring the fluorescence lifetimes of concentrated solutions in the 1 cm cell, because the lifetimes are affected by the reabsorption effect.

As shown in Fig. 3(b), the reabsorption effect can be eliminated by using the 12 μm cell. Therefore, $k_{form}$ can be obtained from the lifetime measurements using this cell. For the concentrated solutions in the 12 μm cell, fluorescence

Table 1
Fluorescence lifetime of perylene in toluene

| Concentration (M) | $\tau_f^M$ (1 cm cell) ($10^{-9}$ s) | | | $\tau_f^M$ (12 μm cell) ($10^{-9}$ s) | | |
|---|---|---|---|---|---|---|
| | 445 nm | 470 nm | 500 nm | 445 nm | 470 nm | 500 nm |
| $2.4 \times 10^{-6}$ | 4.6 | 4.6 | 4.6 | – | – | – |
| $0.4 \times 10^{-3}$ | 5.7 | 6.1 | 6.2 | 4.5 | 4.5 | 4.5 |
| $2.0 \times 10^{-3}$ | 5.2 | 5.8 | 6.0 | 4.3 | 4.3 | 4.3 |
| $2.8 \times 10^{-3}$ | 5.1 | 5.7 | 5.9 | 4.2 | 4.2 | 4.2 |
| $4.7 \times 10^{-3}$ | 4.8 | 5.4 | 5.7 | 3.9 | 3.9 | 3.9 |

lifetime does not depend on the observation wavelength at any concentration. The result using the 12 μm cell is consistent with Eq. (2), namely, the lifetime obtained by extrapolating to zero concentration coincides with that in the dilute solution. Hence, from this result, the rate constant $k_{form}$ of excimer formation can be obtained to be $8 \times 10^9\,M^{-1}\,s^{-1}$.

The rate constant, $k_{dif}$, of the diffusion-controlled reaction between the same molecules can be expressed as [1]

$$k_{dif} = \frac{8RT}{3\eta} \quad (3)$$

where $\eta$ is the viscosity of the solvent. Using the value of $\eta = 0.59 \times 10^{-3}$ Pa s at 293 K [23] for toluene, $k_{dif}$ is calculated to be $1.1 \times 10^{10}\,M^{-1}\,s^{-1}$. Thus, we can conclude that the excimer formation of perylene is almost diffusion-controlled. For many aromatic molecules, excimer formation in fluid solution is reported to be diffusion-controlled [1].

### 3.3. Observation of excimer fluorescence

Excimer fluorescence of aromatic molecules has been observed in the longer wavelength range compared to monomer fluorescence [1]. Fig. 7 shows the fluorescence spectra of a concentrated solution ($4.7 \times 10^{-3}$ M) in the 12 μm cell and of a dilute solution ($2.4 \times 10^{-6}$ M) in the 1 cm cell after normalization at 550 nm. The spectrum obtained by subtracting the spectrum of the dilute solution from that of the concentrated solution is also shown. The spectrum is broad and structureless with the peak around 640 nm ($E_f^D = 1.94$ eV). The shape and the peak position of the band are similar to those in crystals (peak: 590 nm) [12] and LB-films (peak: 605 nm) [14]. Thus, we assign the observed spectrum to excimer fluorescence. Rigorously speaking, the peak position of the excimer fluorescence in solution is slightly red-shifted. This implies that perylene excimer in solution has a more stable structure than those in crystal and in LB-film.

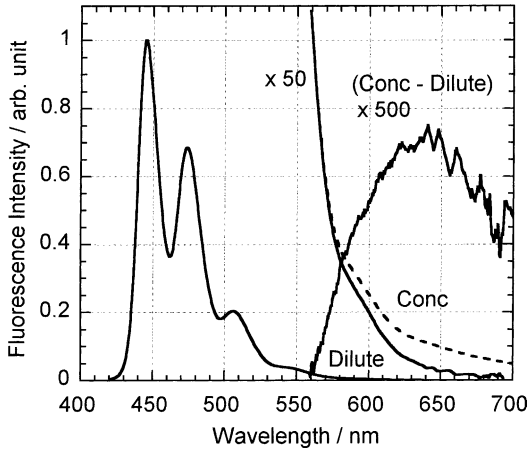


Fig. 7. Fluorescence spectra of a dilute solution ($2.4 \times 10^{-6}$ M) in a 1 cm cell (solid line) and of a concentrated solution ($4.7 \times 10^{-3}$ M) in a 12 μm cell (dashed line). The spectra are normalized at 550 nm. The fluorescence spectrum obtained by subtracting the spectrum of the dilute solution from that of the concentrated solution is also shown.

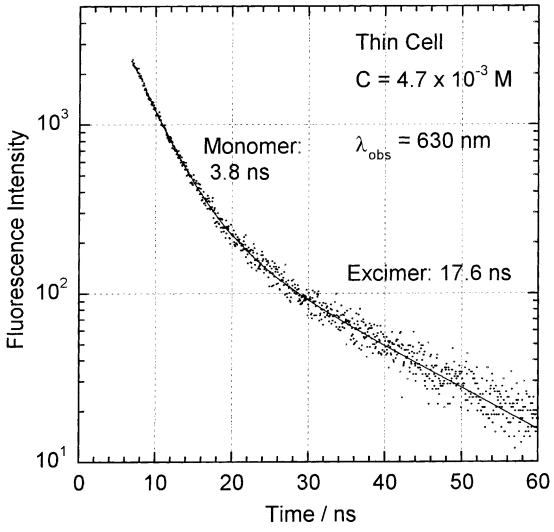


Fig. 8. Fluorescence decay profile of a concentrated solution ($4.7 \times 10^{-3}$ M) observed at 630 nm (dots: observed decay profile; solid line: fitted decay profile).

To analyze the formation and decay processes of perylene excimer in more detail, we measured the fluorescence decay in a concentrated solution ($4.7 \times 10^{-3}$ M) at 630 nm using the 12 μm cell at 293 K (Fig. 8). As shown in Fig. 4, the decay profile of a concentrated solution observed at 470 nm (monomer fluorescence) can be fitted by a single exponential function. On the contrary, the fluorescence decay curve of the concentrated solution (Fig. 8) monitored at 630 nm is not a single exponential function but is represented by a double exponential function. The fast decay component (3.8 ns) can be assigned to the monomer fluorescence, because its lifetime coincides with that in a concentrated solution observed at 470 nm (3.9 ns). The lifetime of the slow decay component (17.6 ns) is similar to that of the excimer estimated through nanosecond time-resolved transient absorption spectroscopy [15]. We, therefore, assign the long component to the excimer fluorescence. According to a general analysis of the temporal decay of excimer fluorescence [1], monomer fluorescence rises up immediately and decays exponentially. Excimer fluorescence rises up concurrently with the decay of monomer fluorescence. In the present study, however, the rise-up of the excimer fluorescence was not observed, probably because the stronger monomer fluorescence masks the rise-up part of the excimer fluorescence.

### 3.4. Binding energy of excimer

The formation and decay processes of excimer under steady-state condition can be expressed by the following two equations (see Fig. 5):

$$\frac{d[M^*]}{dt} = I_0 - k_f^M[M^*] - k_{form}[M][M^*] + k_{dis}[D^*] = 0 \quad (4)$$

$$\frac{d[D^*]}{dt} = k_{form}[M][M^*] - k_f^D[D^*] - k_{dis}[D^*] = 0 \quad (5)$$

where $I_0$ is the generation term of monomer excited state by light irradiation, [M*] and [D*] refer to the excited monomer and excimer concentrations, respectively. The temperature dependence of the rate constants of the formation $k_{form}$ and dissociation $k_{dis}$ of excimer can be expressed as

$$k_{form} = k_{form}^0 \exp\left(-\frac{E_a^{form}}{kT}\right) \quad (6)$$

$$k_{dis} = k_{dis}^0 \exp\left(-\frac{E_a^{dis}}{kT}\right) \quad (7)$$

where $k^0$'s are the frequency factors and $E_a$'s are the activation energies. They are assumed to be independent of temperature. The formation of excimer is diffusion-controlled and, therefore, $k_{form}^0$ and $E_a^{form}$ can be evaluated from the temperature dependence of the viscosity of the solvent using Eq. (3). In this way, we obtained $k_{form}^0 = 1.14 \times 10^{12}\,M^{-1}\,s^{-1}$ and $E_a^{form} = 0.117\,eV$.

From Eqs. (5)–(7), we obtain following relation:

$$\frac{[D^*]}{[M^*]} = \frac{k_{form}^0 \exp(-(E_a^{form}/kT))}{k_f^D + k_{dis}^0 \exp(-(E_a^{dis}/kT))}[M] \quad (8)$$

In the high temperature limit where $k_{form}[M]$, $k_{dis} \gg k_f^D$, the reaction reaches dynamical equilibrium. Therefore, the equilibrium constant $K$ can be expressed as [1]

$$K = \frac{[D^*]}{[M^*][M]} = \frac{k_{form}^0}{k_{dis}^0} \exp\left[-\frac{E_a^{form} - E_a^{dis}}{kT}\right] = \frac{k_{form}^0}{k_{dis}^0} \exp\left[\frac{E_B}{kT}\right] \quad (9)$$

where $E_B$ is the binding energy of the excimer. In Eq. (9), we take a 1 M solution as the standard state. From the general thermodynamic relations, $K$ can be given as

$$K = \exp\left(-\frac{\Delta G}{RT}\right) = \exp\left(\frac{\Delta S}{R}\right) \exp\left(-\frac{\Delta H}{RT}\right) \quad (10)$$

where $\Delta G$ is the Gibbs free energy change, $\Delta S$ the entropy change and $\Delta H$ the enthalpy change associated with excimer formation. By comparing Eq. (9) with Eq. (10), $k_{dis}^0$ can be estimated. In many aromatic excimers $-\Delta S$ was reported to be $80\,J\,mol^{-1}\,K^{-1}$ [1,5]. We assume that the entropy change has the same value as perylene excimer. Thus, $k_{dis}^0 = 1.7 \times 10^{16}\,s^{-1}$ can be obtained using the estimated value of $k_{form}^0$.

Fig. 9 shows the transient absorption spectrum of a dilute solution of perylene ($10^{-5}$ M). At this concentration, the formation of excimer can be neglected and, therefore, the peak at 710 nm can be assigned to the absorption of the monomer excited state of perylene. Fig. 9 also shows the transient absorption spectra of a concentrated solution ($4.7 \times 10^{-3}$ M) at 292 and 332 K. These spectra were normalized at 710 nm. In both spectra, an additional peak appears at 605 nm and it can be assigned to the absorption due to the excimer [15]. It may be seen that the shape and intensity of the excimer band are not sensitive to temperature. The transient absorption spectra shown in Fig. 9 were recorded using a CCD camera equipped with an electronic gate. In this measurement, the gate width (60 ns) is much longer than the lifetimes of the monomer excited state (3.9 ns) and of the excimer (17.6 ns) so that these spectra can be considered as the absorption spectra of these species integrated over their lifetimes.

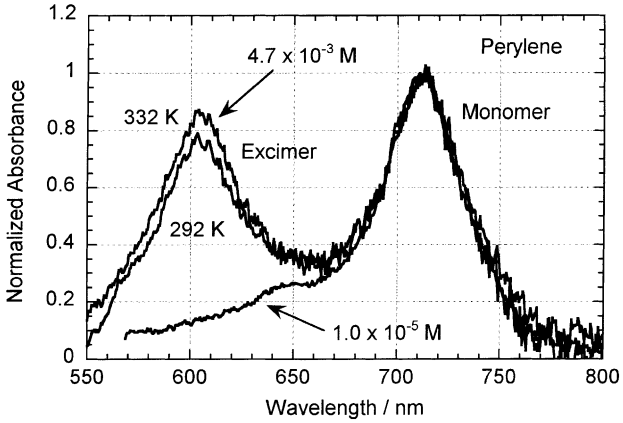


Fig. 9. Transient absorption spectra of perylene in dilute solution ($1.0 \times 10^{-5}$ M) at 292 K and concentrated ($4.7 \times 10^{-3}$ M) solution at 292 and 332 K. These spectra are normalized at 710 nm.

Since, we obtained the values of the parameters $k_{form}^0$, $k_{dis}^0$, $k_f^D$ and $E_a^{form}$ involved in Eq. (8), we can calculate the ratio ([D*]/[M*]) for perylene as a function of temperature and $E_a^{dis}$. The solid lines in Fig. 10 show

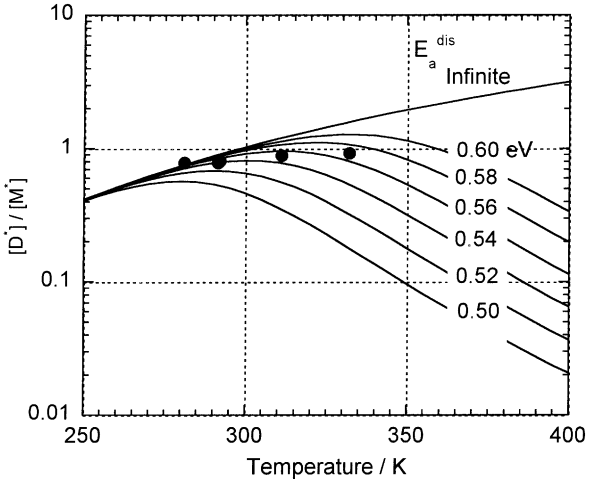


Fig. 10. [D*]/[M*] as a function of temperature. The solid lines give the calculated values from Eq. (8) using several values of $E_a^{dis}$.

([D*]/[M*]) calculated from Eq. (8) for various $E_a^{dis}$ as a function of temperature. The ratio of the peak height of transient absorption (Fig. 9) between the monomer excited state (710 nm) and the excimer (605 nm) gives relative value of ([D*]/[M*]). As shown in Fig. 9, the absorption spectrum of the monomer excited state is overlapped with that of the excimer at 605 nm and, therefore, we subtracted the contribution of the monomer excited state from the spectrum observed for calculation of relative value of ([D*]/[M*]). For the perylene excimer, the absorption coefficients of the monomer excited state and the excimer are not available so that absolute value of ([D*]/[M*]) cannot be obtained directly from transient absorption spectra. By fitting calculated curves with the experimental data shown by closed circles ([D*]/[M*]) and $E_a^{dis}$ can be estimated to be 0.82 at 292 K and 0.56 eV, respectively. It should be noted that the simulated curve using $E_a^{dis} = 0.56$ eV converges to the curve of infinite activation energy around room temperature. This clearly shows that thermal dissociation of perylene excimer is not important at room temperature. It is consistent with the observation that the fluorescence decay shown in Fig. 4 can be fitted to a single exponential function. Using the values of $E_a^{dis} = 0.56$ eV and $E_a^{form} = 0.117$ eV, $E_B$ can be estimated to be 0.44 eV ($-\Delta H = 42\,kJ\,mol^{-1}$) from Eq. (9).

### 3.5. Quantum yield of excimer fluorescence

Using the parameters obtained in Section 3.4, the quantum yield of excimer fluorescence can be estimated. The ratio of the integrated fluorescence intensities ($I_F^D/I_F^M$) of the excimer and the monomer can be expressed as

$$\frac{I_F^D}{I_F^M} = \frac{k_{rad}^D[D^*]}{k_{rad}^M[M^*]} \tag{11}$$

where, $k_{rad}$'s are the rate constants of radiative decay. The rate constant of radiative decay is given by

$$k_{rad} = \Phi_f k_f \tag{12}$$

where $\Phi_f$ is the quantum yield of fluorescence. Thus, from Eqs. (11) and (12), we obtain the following relation:

$$\frac{I_F^D}{I_F^M} = \frac{\Phi_f^D k_f^D}{\Phi_f^M k_f^M}\frac{[D^*]}{[M^*]} \tag{13}$$

From the spectrum shown in Fig. 7, the ratio ($I_F^D/I_F^M$) is found to be 0.0046. We take $\Phi_f^M$ to be 0.89, which is a reported value for benzene solution [1] and [D*]/[M*] to be 0.82 at 292 K. Accordingly, we can estimate the quantum yield $\Phi_f^D$ of excimer fluorescence as 0.02 and also $\tau_{rad}^D (= 1/k_{rad}^D)$ as 900 ns. The radiative lifetime $\tau_{rad}^D$ of perylene excimer obtained is considerably longer than that of pyrene (86 ns) and similar to that of benzene (1 μs) and 1-methylnaphthalene (900 ns) [1,2]. The long radiative lifetime suggests that perylene excimer has a parallel conformation. This is because in a molecular complex with a parallel conformation consisting of molecules having $D_{2h}$ symmetry such as naphthalene and perylene, the optical transition between the ground state and the lowest excited state becomes symmetrically forbidden.

### 3.6. Estimation of the transfer integral V

According to the Mulliken–Hush theory, the transfer integral (the electronic coupling matrix element by the charge transfer interaction) $V$ between a neutral excited state and an ion-pair state can be expressed as Eq. (14) [24], where the peak position $\nu_{MAX}$ and FWHM $\Delta\nu_{1/2}$ of charge transfer band are in unit of wavenumbers, the absorption coefficient $\varepsilon_{MAX}$ in $mol^{-1}\,dm^3\,cm^{-1}$ and the separation $r_D$ between molecules is in angstroms:

$$V = \frac{2.06 \times 10^{-2}(\nu_{MAX}\varepsilon_{MAX}\Delta\nu_{1/2})^{1/2}}{r_D} \tag{14}$$

The transfer integral $V$ can be evaluated if the absorption coefficient and the band shape are available.

The absorption coefficients of the monomer excited state of perylene can be estimated by transient absorption spectroscopy. We carefully measured the exciting light intensity and the overlap between the exciting light beam and the probe light beam for the transient absorption measurements in the dilute solution of perylene. As a result, the absorption coefficient of the monomer excited state at 710 nm was estimated to be $\varepsilon_{M^*}^{710} = 17{,}000\,mol^{-1}\,dm^3\,cm^{-1}$. In the transient absorption spectrum of the concentrated solution, the absorption spectrum of the excimer can be observed as shown in Fig. 9. From the relation

$$\frac{A_{D^*}^{605}}{A_{M^*}^{710}} = \frac{\varepsilon_{D^*}^{605}}{\varepsilon_{M^*}^{710}}\frac{[D^*]}{[M^*]} \tag{15}$$

we obtain the absorption coefficient $\varepsilon_{D^*}^{605}$ of the excimer at 605 nm using the value of ([D*]/[M*]) = 0.82 at 292 K which has been obtained from Fig. 10. Actually, the absorption spectrum of the excimer is overlapped with that of the monomer excited state at 605 nm and, therefore, the contribution from the monomer excited state has to be subtracted for the evaluation of absorbance ratio $A_{D^*}^{605}/A_{M^*}^{710}$. As a result, the absorption coefficient of the excimer can be estimated to be $\varepsilon_{D^*}^{605} = 15{,}000\,mol^{-1}\,dm^3\,cm^{-1}$.

Fig. 11 shows the transient absorption spectrum of a concentrated solution ($4.7 \times 10^{-3}$ M) of perylene over a wide wavelength range. We recorded the spectrum just after excitation, so that the spectrum is not an integrated one over the lifetimes of the excimer and the monomer excited state. Therefore, the peak height of the excimer compared with that of the monomer excited state is slightly smaller than that in Fig. 9. In the shorter wavelength range, the peaks of both the excimer (605 nm) and the monomer excited state (710 nm) are observed. In the near-IR range an additional peak around 1350 nm can be observed. This peak is assigned to the charge transfer transition of the

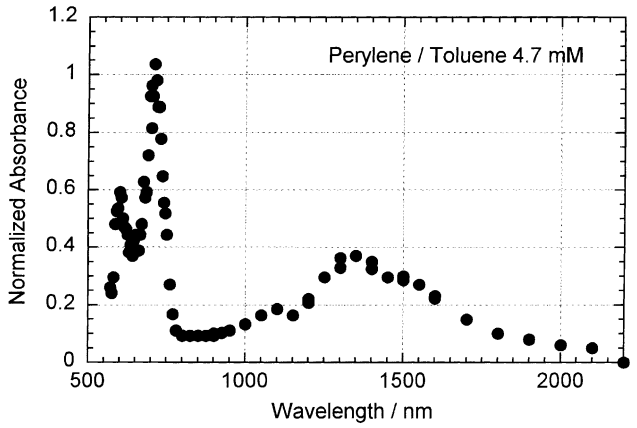


Fig. 11. Transient absorption spectrum of perylene in concentrated solution ($4.7 \times 10^{-3}$ M) in the wavelength range 550–2200 nm.

excimer [16]. The absorption coefficient $\varepsilon_{D^*}^{1350}$ at 1350 nm can be estimated by comparing its absorption intensity with that at 605 nm. As a result, $\varepsilon_{D^*}^{1350}$ was estimated to be 12,000 $mol^{-1}\,dm^3\,cm^{-1}$. Using the values of $\nu_{MAX} = 7400\,cm^{-1}$, $\varepsilon_{MAX} = 12{,}000\,mol^{-1}\,dm^3\,cm^{-1}$, $\Delta\nu_{1/2} = 2600\,cm^{-1}$ and $r_D = 0.33$ nm, the transfer integral $V$ can be estimated to be 0.37 eV.

At present, few attempts have been made to estimate $V$ of charge transfer complexes in excited states, so that it is difficult to discuss the relation between the transfer integral and the molecular structures of a donor and an acceptor. Mataga [25] reported the transfer integral $V$ of molecular complexes in the excited state of 1-cyanonaphthalene–naphthalene exciplex to be 0.4–0.5 eV from the analysis of exciplex fluorescence. Gould et al. [26] also estimated $V$ to be 0.167 eV for tetracyanoanthracene–alkylbenzene and 0.161 eV for dicyanoanthracene–alkylbenzene exciplexes from the analysis of absorption and fluorescence spectrum. It seems that $V = 0.37$ eV estimated for perylene excimer is similar to those of exciplexes reported.

According to the perturbation theory, the transition energy $E_{CT}$ of CT absorption band can be expressed as

$$E_{CT} = E_0 \left(1 + \frac{4V^2}{E_0^2}\right)^{1/2} \tag{16}$$

$$E_0 = E_{IP} - E_{exciton} \tag{17}$$

where $E_0$ is the energy difference between an exciton state $E_{exciton}$ and an ion-pair state $E_{ion}$ shown in Fig. 1. We observed the peak of charge transfer band at 0.92 eV (1350 nm) and estimated $V$ as 0.37 eV. Thus, the energy difference $E_0$ between an exciton state and an ion-pair state is found to be 0.55 eV. As shown in Fig. 9, the absorption band of the excimer is not similar to a cation (546 nm [27]) and an anion (578 nm [27]) absorption bands. Therefore, the initial state (fluorescent state) of the near-IR transition can be considered as the neutral electronic state.

### 3.7. Origin of the stabilization energy of perylene excimer

As given in Eq. (1), the binding energy $E_B$ of excimer can be expressed by three contributions: the repulsion energy $E_R$, the stabilization energy by the charge transfer interaction $E_S^{CT}$ and by the exciton interaction $E_S^{exc}$. The repulsion energy $E_R$ of excimer formation has not been estimated experimentally. However, theoretical estimation of the repulsion energy has been made [3,28]. Thus, we assume $E_R = 0.2$ eV. The stabilization energy by the CT interaction can be evaluated from the peak position $E_{CT}$ of the near-IR band and the energy difference between the excimer state and the ion-pair state $E_0$ as follows:

$$E_S^{CT} = \tfrac{1}{2}(E_{CT} - E_0) \tag{18}$$

In Section 3.6, we estimated $E_0 = 0.55$ eV for perylene excimer and $E_{CT} = 0.92$ eV from the peak position of the near-IR absorption of the excimer. Thus, $E_S^{CT}$ can be evaluated to be 0.19 eV. Using these values, $E_S^{exc}$ can be evaluated from Eq. (1) to be 0.45 eV. This shows that the stabilization of perylene excimer is mainly due to the exciton interaction (70%) and a small contribution comes from the CT interaction (30%).

The photophysical parameters and the energy levels obtained in this study are summarized in Fig. 12. Monomer excited state of perylene emits strong fluorescence around 445 nm ($E_f^M = 2.79$ eV). The lifetime of the monomer excited state was obtained as $\tau_f^M = 4.6$ ns. Perylene excimer is efficiently formed with the diffusion-limited rate ($k_{form} = 8 \times 10^9\,M^{-1}\,s^{-1}$). Weak excimer fluorescence ($\Phi_f^D = 0.02$) can be observed around 640 nm ($E_f^D = 1.94$ eV) with lifetime of $\tau_f^D = 17.6$ ns. The excimer is significantly stable and the binding energy was estimated as $E_B = 0.44$ eV. The transfer integral $V$ between a neutral exciton state and an ion-pair state was estimated as $V = 0.37$ eV from the analysis of the near-IR absorption band at 1350 nm ($E_{CT} = 0.92$ eV). Thus, the energy difference $E_0$ between a neutral excited state and an ion-pair state was estimated as $E_0 = 0.55$ eV. From these results, the stabilization energies by the charge transfer and the exciton interactions were estimated as $E_S^{CT} = 0.19$ eV and $E_S^{exc} = 0.45$ eV, respectively.

### 3.8. Comparison with other aromatic excimers

In this section, we discuss the contribution of the charge transfer interaction to the stabilization energy in other aromatic excimers, i.e., benzene, toluene, naphthalene, 1-methylnaphthalene, anthracene, pyrene and 1,12-benzoperylene. As shown in Fig. 1, the charge transfer interaction comes from the mixing between the exciton state and the ion-pair state. The stabilization energy due to the charge transfer interaction can be estimated from Eq. (18) when the energy gap $E_0$ between the exciton state and the

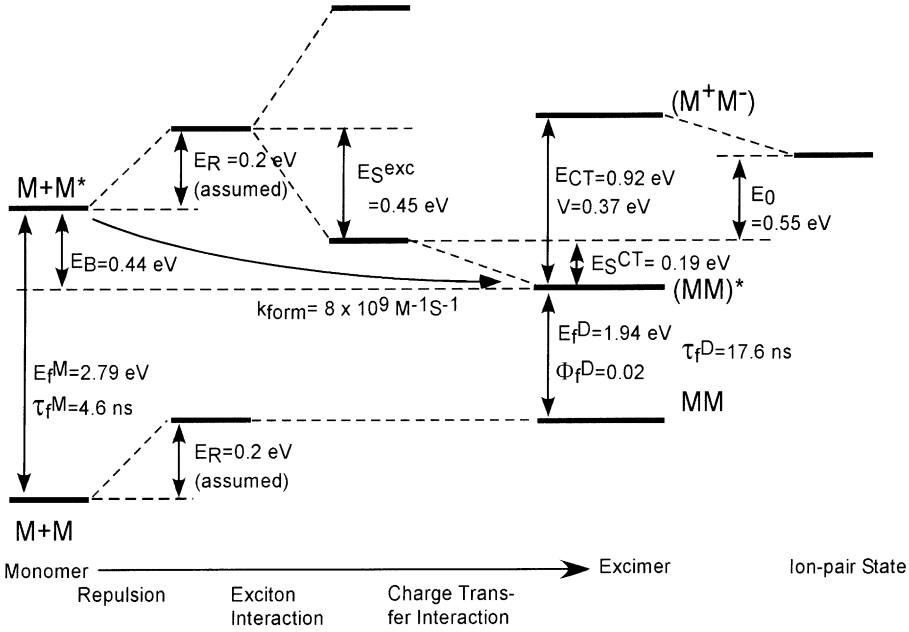


Fig. 12. Photophysical parameters and the energy levels of perylene excimer obtained in this study.

ion-pair state is known. As shown in Fig. 1, the energy $E_{\text{exciton}}$ of the exciton state in Eq. (17) can be expressed as

$$E_{\text{exciton}} = E_{\text{f}}^{\text{D}} + E_{\text{S}}^{\text{CT}} \tag{19}$$

Using Eqs. (16) and (18), $E_{\text{exciton}}$ can be written as

$$E_{\text{exciton}} = E_{\text{f}}^{\text{D}} + \frac{1}{2}\left[E_0\left(1 + \frac{4V^2}{E_0^2}\right)^{1/2} - E_0\right] \tag{20}$$

The energy $E_{\text{IP}}$ of the ion-pair state in Eq. (17) is estimated on the basis of the model presented previously [16]. The ion-pair can be considered as a pair state of a cation and an anion which are separated by the distance $r_{\text{D}}$, so that we estimate the energy of the ion-pair state $E_{\text{IP}}^{\text{calc}}$ using the relation

$$E_{\text{IP}}^{\text{calc}} = I_{\text{g}} - E_{\text{A}} + P_+ + P_- + C \tag{21}$$

where $I_{\text{g}}$ is the ionization potential of a molecule in the gas phase, $E_{\text{A}}$ the electron affinity in the gas phase, $P_+$ and $P_-$ are the polarization energies induced by a cation and an anion, respectively, and $C$ is the Coulomb interaction energy. $I_{\text{g}}$'s and $E_{\text{A}}$'s of the compounds studied are available from literature and the polarization energy $P$ can be estimated by Born's formula [29]

$$P = P_+ = P_- = -\frac{e^2}{8\pi\varepsilon\varepsilon_0 R}\left[1 - \left(\frac{1}{\varepsilon}\right)\right] \tag{22}$$

where $e$ is the elementary charge, $\varepsilon$ the dielectric constant of the medium, $\varepsilon_0$ the permitivity of the vacuum and $R$ the effective radius of the ion. It has been known that Born's formula gives reasonable values when the van der Waals radius $R_{\text{vdW}}$ [30] is used as the effective radius $R$ of the ion [31]. Therefore, we take $R_{\text{vdW}}$ of the molecules studied as the effective radius of the corresponding ions. We use the square of the refractive index $n^2$ as $\varepsilon$ because the solvent used is nonpolar. The magnitude of $C$ can be estimated as

$$C = -\frac{e^2}{4\pi\varepsilon\varepsilon_0 r_{\text{D}}} \tag{23}$$

The distance was assumed to be $r_{\text{D}} = 0.33\,\text{nm}$ following the theoretical calculation of naphthalene excimer [28]. Thus, we can estimate the energy $E_{\text{IP}}^{\text{calc}}$ of the ion-pair state.

Quantitative discussion of $E_0$ estimated using the above model is not easy because of its oversimplification. Therefore, we add the correction factor $F$ to the expression of $E_0$. From Eqs. (17) and (20), we obtain following relation:

$$E_0^{\text{calc}} = \frac{(E_{\text{IP}}^{\text{calc}} - E_{\text{f}}^{\text{D}} + F)^2 - V^2}{E_{\text{IP}}^{\text{calc}} - E_{\text{f}}^{\text{D}} + F} \tag{24}$$

In the case of perylene, we already estimated $V = 0.37\,\text{eV}$ and $E_0 = 0.55\,\text{eV}$ in Section 3.6. From these values, the correction factor $F$ can be evaluated to be $F = 0.93$. Therefore, $E_0$ for other excimers can be estimated if we assume the transfer integral $V$.

Fig. 13 shows the peak position $E_{\text{CT}}^{\text{obs}}$ of the charge transfer absorption in aromatic excimers as a function of the energy difference $E_0^{\text{calc}}$. In the calculation, we assumed that $V$ is the same as that of perylene ($V = 0.37\,\text{eV}$). In Table 2, the values calculated are listed. It seems that $E_{\text{CT}}^{\text{obs}}$ deviates from the straight line (dashed line in Fig. 13, $E_0^{\text{calc}} = E_{\text{CT}}^{\text{obs}}$) at small $E_0^{\text{calc}}$. This clearly shows that the contribution of $E_{\text{S}}^{\text{CT}}$ to the stabilization energy of excimers is important. The solid

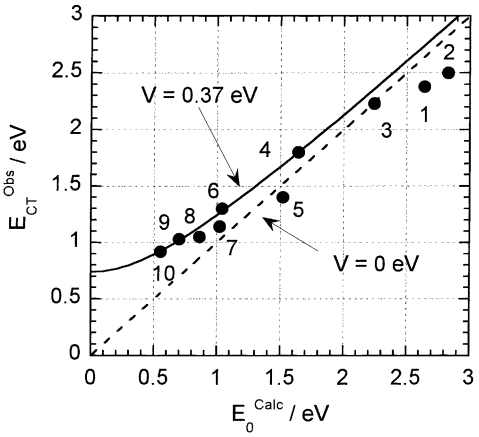


Fig. 13. The peak energy of the near-IR absorption band of various excimers as a function of $E_0^{calc}$. A number in the figure represents the compounds listed in Table 2. Dashed line: no contribution from the charge transfer interaction. Solid line: the peak position calculated from Eq. (16) using the value of $V = 0.37\,eV$.

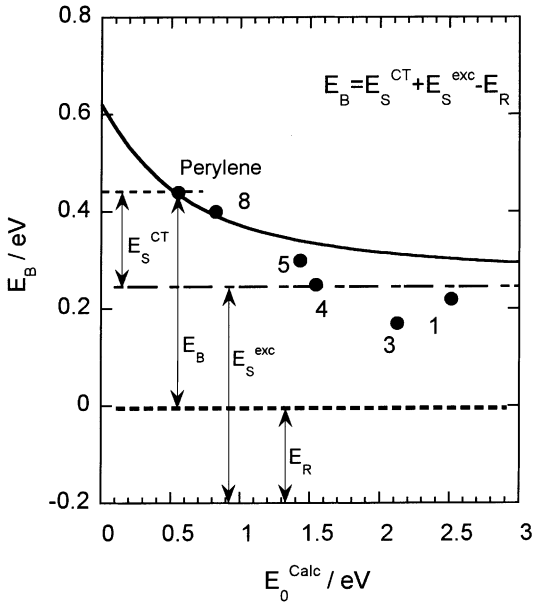


Fig. 14. The binding energy $E_B$ of aromatic excimers as a function of $E_0^{calc}$. The origin of the binding energy of excimer is also shown schematically using the constant value of $E_S^{exc} = 0.45\,eV$ and $E_R = 0.2\,eV$.

curve in Fig. 13 shows the peak position estimated from Eq. (16) using the value of $V = 0.37\,eV$. At small $E_0^{calc}$, the peak energies are well fitted by the solid line. This indicates that these excimers have a similar transfer integral $V$.

As we discussed, the contribution of the charge transfer interaction to the stabilization energy of excimer decreases with decreasing size of the molecule. In order to discuss the origin of the stabilization energy in various aromatic excimers, we plot the reported values of the binding energy

Table 2
Parameters for estimation of $E_0$

| No. | Compound | Solvent | $I_g$[a,b] (eV) | $E_A$[c,d,e] (eV) | $P$[f] (eV) | $R_{vdW}$[g] (nm) | $n^2$[h] | $C$[i] (eV) | $E_{IP}^{calc}$[j] (eV) | $E_f^D$[k,d] (eV) | $E_0^{calc}$[l] (eV) | $E_{CT}^{obs}$[m,n] (eV) | $E_b$[o] (eV) |
|---|---|---|---|---|---|---|---|---|---|---|---|---|---|
| 1 | Benzene | Liquid | 9.17 | −1.40 | −1.51 | 0.268 | 2.28 | −1.91 | 6.57 | 3.88 | 2.64 | 2.38 | 0.22 |
| 2 | Benzene | Cyclohexane | 9.17 | −1.40 | −1.36 | 0.268 | 2.02 | −2.16 | 6.63 | 3.75 | 2.83 | 2.50 | 0.22 |
| 3 | Toluene | Liquid | 8.67 | −1.30 | −1.39 | 0.286 | 2.23 | −1.96 | 6.17 | 3.87 | 2.24 | 2.23[p] | 0.17 |
| 4 | Naphthalene | Gas | 8.12 | −0.20 | 0.00 | 0.309 | 1.00 | −4.36 | 4.89 | 3.17 | 1.64 | 1.80 | 0.25 |
| 5 | 1-Methylnaphthalene | Liquid | 7.95 | −0.20 | −1.38 | 0.323 | 2.62 | −1.66 | 4.66 | 3.05 | 1.52 | 1.40 | 0.25 |
| 6 | Anthracene | Liquid | 7.36 | 0.60 | −1.43 | 0.341 | 3.12 | −1.40 | 3.42 | 2.27[q] | 1.04 | 1.30 | |
| 7 | Anthracene | Benzene | 7.36 | 0.60 | −1.18 | 0.341 | 2.28 | −1.91 | 3.41 | 2.27 | 1.02 | 1.14 | |
| 8 | Pyrene | Cyclohexane | 7.37 | 0.50 | −1.03 | 0.352 | 2.02 | −2.16 | 3.58 | 2.58 | 0.86 | 1.05 | 0.4 |
| 9 | 1,12-Benzoperylene | Toluene | 7.12 | 0.60 | −1.03 | 0.386 | 2.23 | −1.96 | 3.44 | 2.58 | 0.70 | 1.03[r] | |
| 10 | Perylene | Toluene | 6.90 | 1.10 | −1.05 | 0.378 | 2.23 | −1.96 | 2.67 | 1.94[s] | 0.55 | 0.92[s] | 0.44 |

[a] Ionization potential in the gas phase.
[b] Ref. [32].
[c] Electron affinity in the gas phase.
[d] Ref. [1].
[e] Ref. [6].
[f] Polarization energy.
[g] van der Waals radius.
[h] Refractive index of the solvent.
[i] Coulomb energy.
[j] Energy of ion-pair state calculated.
[k] Peak energy of excimer fluorescence.
[l] Energy difference between an exciton state and an ion-pair state calculated from Eq. (24).
[m] Peak energy of charge transfer band observed.
[n] Ref. [16].
[o] Binding energy of excimer.
[p] Ref. [33].
[q] The value for benzene solution.
[r] Ref. [34].
[s] Present result.

$E_B(= E_S^{exc} + E_S^{CT} - E_R)$ of excimer as a function of $E_0^{calc}$ in Fig. 14. It seems that $E_B$ decreases with decreasing the size of the molecule. This indicates that the decrease in the charge transfer interaction is at least partly responsible for the decrease of the binding energy of excimer. The solid line in Fig. 14 shows $E_B$ evaluated using the constant values of $E_S^{exc} = 0.45\,eV$ and $E_R = 0.2\,eV$. In the case of small molecules, $E_B$ observed is smaller than that estimated. This suggests that the stabilization energy $E_S^{exc}$ of exciton interaction decreases with decreasing molecular size.

## 4. Conclusion

We study the origin of the stabilization energy of perylene excimer in toluene through fluorescence and transient absorption spectroscopy. In order to eliminate the reabsorption effect, we designed a thin optical cell with a path length of about 10 μm for the precise measurements of the fluorescence decay profiles and the spectra (Section 3.1). From the measurement of decay profile of the fluorescence of monomer excited state using the thin cell, it was found that the excimer formation is almost diffusion-controlled (Section 3.2). In longer wavelength range of the fluorescence spectrum, we can measure very weak excimer fluorescence spectrum. We also observed fluorescence decay of the excimer fluorescence (Section 3.3). From the result of temperature dependence of the transient absorption, the binding energy of perylene excimer can be estimated (Section 3.4). Using the photophysical parameters obtained, we estimated the quantum yield of the excimer fluorescence (Section 3.5). In the near-IR wavelength range, the charge transfer absorption band of excimer can be observed. By analyzing the band shape, the transfer integral $V$ between a neutral exciton state and an ion-pair state can be estimated (Section 3.6). From these results, we conclude that the stabilization energy of perylene excimer consists of two components: exciton interaction (70%) and charge transfer interaction (30%) (Section 3.7). We discuss the origin of the stabilization energy of other aromatic excimers on the basis of the results on perylene excimer (Section 3.8).

## Acknowledgements

We are grateful to Professor Jiro Tanaka for helpful discussions. This work was supported by COE development project of Science and Technology Agency of Japan.

## References

[1] J.B. Birks, Photophysics of Aromatic Molecules, Wiley, New York, 1970.
[2] J.B. Birks, Rep. Prog. Phys. 38 (1975) 903.
[3] J.N. Murrell, J. Tanaka, J. Mol. Phys. 4 (1964) 363.
[4] T. Azumi, A. Armstrong, J. McGlynn, J. Chem. Phys. 41 (1964) 3839.
[5] B. Stevens, Adv. Photochem. 8 (1971) 161.
[6] M. Pope, C.E. Swenberg, Electronic Processes in Organic Crystals, Clarendon Press, Oxford, 1982, p. 204.
[7] Z.D. Popovic, R.O. Loutfy, A.-M. Hor, Can. J. Chem. 63 (1985) 134.
[8] S. Ferrere, A. Zaban, B.A. Gregg, J. Phys. Chem. B 101 (1997) 4490.
[9] M. Hoffmann, K. Schmidt, T. Frita, T. Hasche, V.M. Agranovich, K. Leo, Chem. Phys. 258 (2000) 73.
[10] G. Mazur, P. Petelentz, Chem. Phys. Lett. 324 (2000) 161.
[11] J.B. Birks, L.G. Christophorou, Proc. R. Soc. A 277 (1964) 571.
[12] B. Walker, H. Port, H.C. Wolf, Chem. Phys. 92 (1985) 177.
[13] M. Mataga, Y. Torihashi, Y. Ota, Chem. Phys. Lett. 1 (1967) 385.
[14] J. Mahrt, F. Willig, W. Storck, D. Weiss, R. Kietzmann, K. Schwarzburg, B. Tufts, B. Trösken, J. Phys. Chem. 98 (1994) 1888.
[15] C.R. Goldschmidt, M. Ottolenghi, J. Phys. Chem. 75 (1971) 3894.
[16] R. Katoh, E. Katoh, N. Nakashima, M. Yuuki, M. Kotani, J. Phys. Chem. A 101 (1997) 7725.
[17] A. Penzkofer, W. Leupacher, J. Lumin. 37 (1987) 61.
[18] W.H. Melhuish, J. Phys. Chem. 65 (1961) 229.
[19] A. Penzkofer, Y. Lu, Chem. Phys. 103 (1986) 399.
[20] M. Kawahigashi, S. Hirayama, J. Lumin. 43 (1989) 297.
[21] S. Murata, M. Nishimura, S.Y. Matsuzaki, M. Tachiya, Chem. Phys. Lett. 219 (1994) 200.
[22] D. Rehm, A. Weller, Isr. J. Chem. 8 (1970) 259.
[23] 60th CRC Handbook of Chemistry and Physics, CRC Press, Boca Raton, FL, 1980.
[24] C. Creutz, M.D. Newton, N. Sutin, J. Photochem. Photobiol. A 82 (1994) 47.
[25] N. Mataga, in: M. Gordon, W.R. Ware (Eds.), The Exciplex, Academic Press, New York, 1975, p. 113.
[26] I.R. Gould, R.H. Young, L.J. Mueller, A.C. Albrecht, S. Farid, J. Am. Chem. Soc. 116 (1994) 8188.
[27] T. Shida, Electronic Absorption Spectra of Radical Ions, Elsevier, Amsterdam, 1988.
[28] R.G. Sadygov, E.C. Lim, Chem. Phys. Lett. 225 (1994) 441.
[29] M. Born, Z. Phys. 1 (1920) 45.
[30] J.T. Edward, J. Chem. Ed. 47 (1970) 261.
[31] R. Katoh, K. Lacmann, W.F. Schmidt, Z. Phys. Chem. 190 (1995) 193.
[32] K. Seki, Mol. Cryst. Liq. Cryst. 171 (1989) 255.
[33] H. Miyasaka, H. Masuhara, N. Mataga, J. Phys. Chem. 89 (1985) 1631.
[34] R. Katoh, S. Murata, M. Tachiya, to be published.